Research in Astron. Astrophys. **2012** Vol. **12** No. **12**, 1666–1672
http://www.raa-journal.org *http://www.iop.org/journals/raa*

***R**esearch in*
***A**stronomy and*
***A**strophysics*

Application of a probabilistic neural network in analysis of the radial velocity curve of spectroscopic binary stars

Kamal Ghaderi[1], Kayoomars Karami[2], Ali Pirkhedri[1], Hamid Haj Seyyed Javadi[3] and Touba Rostami[1]

[1] Department of Science and Engineering, Islamic Azad University, Marivan Branch, Marivan, Iran; *K.Ghaderi.60@gmail.com*
[2] Department of Physics, University of Kurdistan, Pasdaran St., Sanandaj, Iran
[3] Department of Mathematics and Computer Science, Faculty of Mathematics and Computer Science, Shahed University, Tehran, Iran

Received 2011 October 12; accepted 2012 June 14

Abstract Using measured radial velocity data of five double-lined spectroscopic binary systems, HD 89959, HD 143705, HD 146361, HD 165052 and HD 152248, we find corresponding orbital and spectroscopic elements via a Probabilistic Neural Network. Our numerical results are in good agreement with those obtained by others using more traditional methods.

Key words: stars: binaries: eclipsing — binaries: spectroscopic (HD 89959, HD 143705, HD 146361, HD 165052 and HD 152248)

1 INTRODUCTION

Analysis of both light and radial velocity (hereafter $V_{\rm R}$) curves of binary systems helps us to determine the masses and radii of individual stars. One historically well-known method to analyze the $V_{\rm R}$ curve is that of Lehmann-Filhés (1894). Some other methods were also introduced by Sterne (1941) and Petrie (1962). The different methods for $V_{\rm R}$ curve analysis have been reviewed in ample detail by Karami & Teimoorinia (2007). Karami & Teimoorinia (2007) also proposed a new non-linear least squares velocity curve analysis technique for spectroscopic binary stars. They showed the validity of applying their new method to a wide range of different types of binary systems (See Karami & Mohebi 2007a,b; Karami et al. 2008 and Karami & Mohebi 2009).

The method of a Probabilistic Neural Network (PNN) is a new tool to derive the orbital parameters of spectroscopic binary stars. In this method, the time consumed is considerably less than the method of Lehmann-Filhés, and even less than the non-linear regression method proposed by Karami & Teimoorinia (2007).

In the present paper, we use a PNN to find the optimum match to four parameters of the $V_{\rm R}$ curves from five double-lined spectroscopic binary systems: HD 89959, HD 143705, HD 146361, HD 165052 and HD 152248. Our aim is to show the validity of applying our new method to a wide range of different types of binary systems.

HD 89959 is a double-lined object with components that are very similar to one another. The spectral type is K0 V with a period of $P = 10.99291$ days (Griffin & Filiz Ak 2010). HD 143705 is double-lined and has components that are almost identical with one another. The spectral type is G0 V with a period of $P = 8.468685$ days (Griffin & Filiz Ak 2010). HD 146361 is a binary in the sigma CrB system. Sigma CrB is a triple system of G0-G1 spectral type. Its period is $P = 1.1397912$ days (Bakos 1984). HD 165052 is a massive binary that probably belongs to the open cluster NGC 6530, in the Lagoon Nebula. The spectral type is O6 and O6.5 for the primary and secondary stars, respectively and the orbital period is $P = 2.95515$ days (Linder et al. 2007). HD 152248 is an O+O binary system that belongs to the young open cluster NGC 6231. The spectral type is O7.5 and O7 for the primary and secondary stars, respectively and the orbital period is $P = 5.816032$ days (Sana et al. 2001).

This paper is organized as follows. In Section 2, we introduce a PNN to estimate the four parameters of the $V_{\rm R}$ curve. In Section 3, the numerical results are reported, while the conclusions are given in Section 4.

2 ESTIMATION OF $V_{\rm R}$ CURVE PARAMETERS BY USING THE PNN

Following Smart (1990), the $V_{\rm R}$ of a star in a binary system is defined as follows

$$V_{\rm R} = \gamma + K[\cos(\theta + \omega) + e\cos\omega], \tag{1}$$

where γ is the $V_{\rm R}$ of the center of mass of the system with respect to the Sun, K is the amplitude of $V_{\rm R}$ of the star with respect to the center of mass of the binary, and θ, ω and e are the angular polar coordinate (true anomaly), the longitude of periastron and the eccentricity, respectively.

Here we apply the PNN method to estimate the four orbital parameters, γ, K, e and ω, of the $V_{\rm R}$ curve in Equation (1). In this work, for the identification of the observational $V_{\rm R}$ curves, the input vector is the fitted $V_{\rm R}$ curve of a star. The PNN is first trained to classify $V_{\rm R}$ curves corresponding to all the possible combinations of γ, K, e and ω. For this, one can synthetically generate $V_{\rm R}$ curves given by Equation (1) for each combination of parameters:

- $-100 \leq \gamma \leq 100$ in steps of 1;
- $1 \leq K \leq 300$ in steps of 1;
- $0 \leq e \leq 1$ in steps of 0.001;
- $0° \leq \omega \leq 360°$ in steps of 5°.

This gives a very large set of k pattern groups, where k denotes the number of different $V_{\rm R}$ classes, one class for each combination of γ, K, e and ω. Since this very large number of different $V_{\rm R}$ classes causes some computational limitations, one can start with large step sizes. Note that from Petrie (1962), one can guess γ, K and e from a $V_{\rm R}$ curve. This enables one to limit the range of parameters around their initial guesses. When the preliminary orbit has been derived after several stages, then one can use the above small step sizes to obtain the final orbit. The PNN has four layers including the input, pattern, summation, and output layers, respectively (see fig. 5 in Bazarghan et al. 2008). When an input vector is presented, the pattern layer computes distances from the input vector to the training input vectors and produces a vector whose elements indicate how close the input is to a training input. The summation layer sums these contributions for each class of inputs to produce as its net output a vector of probabilities. Finally, a competitive transfer function on the output layer picks the maximum of these probabilities, and produces a 1 for that class and a 0 for the other classes (Specht 1988, 1990). Thus, the PNN classifies the input vector into a specific k class labeled by the four parameters γ, K, e and ω because that class has the maximum probability of being correct.

3 NUMERICAL RESULTS

Here, we use the PNN to derive the orbital elements for the five different double-lined spectroscopic systems HD 89959, HD 143705, HD 146361, HD 165052 and HD 152248. Using measured $V_{\rm R}$ data

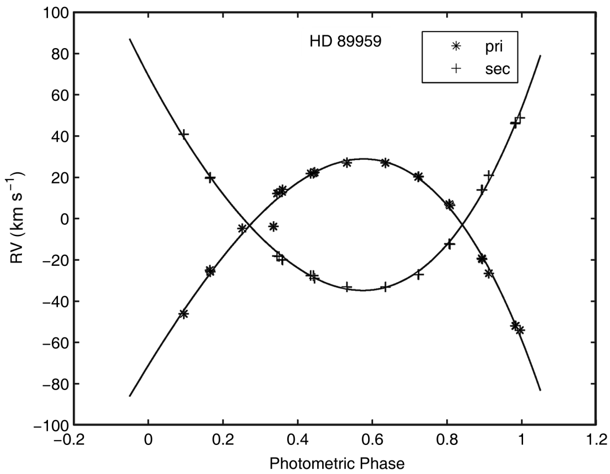

Fig. 1 Radial velocities of the primary and secondary components of HD 89959 plotted against the photometric phase. The observational data have been measured by Griffin & Filiz Ak (2010).

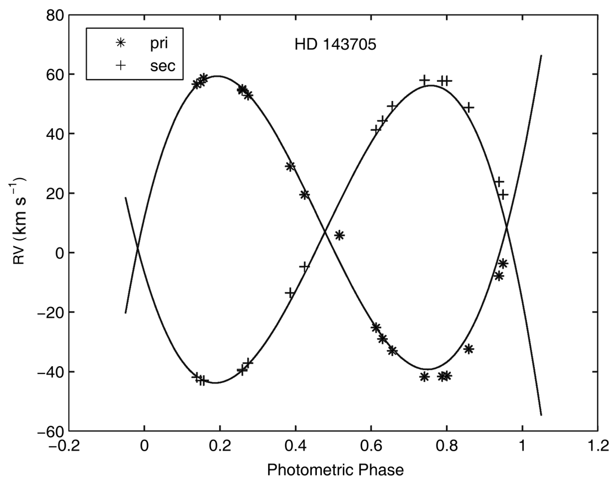

Fig. 2 Radial velocities of the primary and secondary components of HD 143705 plotted against the photometric phase. The observational data have been measured by Griffin & Filiz Ak (2010).

of the two components of these systems obtained by Griffin & Filiz Ak (2010) for HD 89959 and HD 143705, Bakos (1984) for HD 146361, Linder et al. (2007) for HD 165052 and Sana et al. (2001) for HD 152248, the fitted velocity curves are plotted in terms of the photometric phase in Figures 1 to 5.

The orbital parameters obtained from the PNN for HD 89959, HD 143705, HD 146361, HD 165052 and HD 152248 are tabulated in Table 1. This Table shows that the results are in good accordance with those obtained by Griffin & Filiz Ak (2010) for HD 89959 and HD 143705, Bakos (1984) for HD 146361, Linder et al. (2007) for HD 165052 and Sana et al. (2001) for HD 152248.

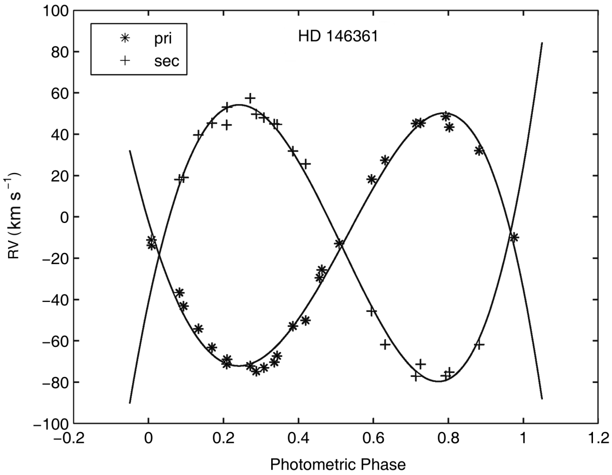

Fig. 3 Radial velocities of the primary and secondary components of HD 146361 plotted against the photometric phase. The observational data have been measured by Bakos (1984).

Table 1 Orbital Parameters of HD 89959, HD 143705, HD 146361, HD 165052 and HD 152248

Name	Parameter	This Paper	Other paper	Reference
HD 89959	$\gamma(\mathrm{km\,s^{-1}})$	-2 ± 1	-2.97 ± 0.03	
	$K_\mathrm{p}(\mathrm{km\,s^{-1}})$	42 ± 1	42.31 ± 0.07	
	$K_\mathrm{s}(\mathrm{km\,s^{-1}})$	43 ± 1	42.68 ± 0.07	Griffin & Filiz Ak (2010)
	e	0.287 ± 0.001	0.2877 ± 0.0011	
	$\omega(^\circ)$	170 ± 5	162.60 ± 0.24	
HD 143705	$\gamma(\mathrm{km\,s^{-1}})$	7 ± 1	7.77 ± 0.07	
	$K_\mathrm{p}(\mathrm{km\,s^{-1}})$	51 ± 1	50.95 ± 0.14	
	$K_\mathrm{s}(\mathrm{km\,s^{-1}})$	52 ± 1	51.59 ± 0.14	Griffin & Filiz Ak (2010)
	e	0.120 ± 0.001	0.1205 ± 0.0017	
	$\omega(^\circ)$	285 ± 5	279.1 ± 1.0	
HD 146361	$\gamma(\mathrm{km\,s^{-1}})$	-12 ± 1	-12.17 ± 1.29	
	$K_\mathrm{p}(\mathrm{km\,s^{-1}})$	64 ± 1	63.42 ± 1.17	
	$K_\mathrm{s}(\mathrm{km\,s^{-1}})$	66 ± 1	65.37 ± 2.67	Bakos (1984)
	e	0.022 ± 0.001	0.022 ± 0.010	
	$\omega(^\circ)$	90 ± 5	85 ± 13	
HD 165052	$\gamma_\mathrm{p}(\mathrm{km\,s^{-1}})$	2 ± 1	2.1 ± 1.2	
	$\gamma_\mathrm{s}(\mathrm{km\,s^{-1}})$	2 ± 1	1.4 ± 1.3	
	$K_\mathrm{p}(\mathrm{km\,s^{-1}})$	97 ± 1	96.4 ± 1.6	Linder et al. (2007)
	$K_\mathrm{s}(\mathrm{km\,s^{-1}})$	114 ± 1	113.5 ± 1.9	
	e	0.081 ± 0.001	0.081 ± 0.015	
	$\omega(^\circ)$	305 ± 5	298.0 ± 10.2	
HD 152248	$\gamma_\mathrm{p}(\mathrm{km\,s^{-1}})$	-30 ± 1	-30.3 ± 1.5	
	$\gamma_\mathrm{s}(\mathrm{km\,s^{-1}})$	-30 ± 1	-28.7 ± 4.3	
	$K_\mathrm{p}(\mathrm{km\,s^{-1}})$	217 ± 1	216.0 ± 1.5	Sana et al. (2001)
	$K_\mathrm{s}(\mathrm{km\,s^{-1}})$	214 ± 1	213.7 ± 5.2	
	e	0.127 ± 0.001	0.127 ± 0.007	
	$\omega(^\circ)$	90 ± 5	84.8 ± 4.7	

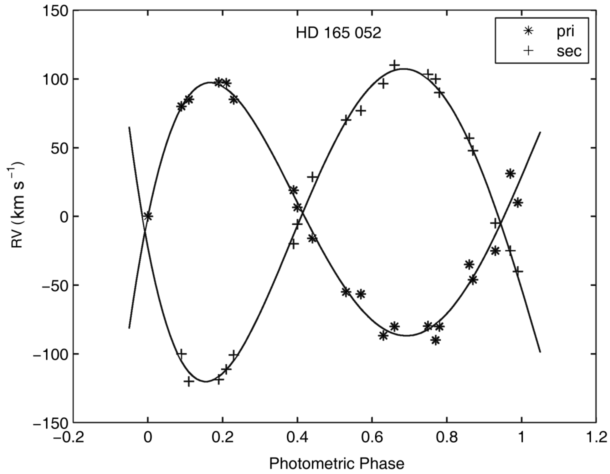

Fig. 4 Radial velocities of the primary and secondary components of HD 165052 plotted against the photometric phase. The observational data have been measured by Linder et al. (2007).

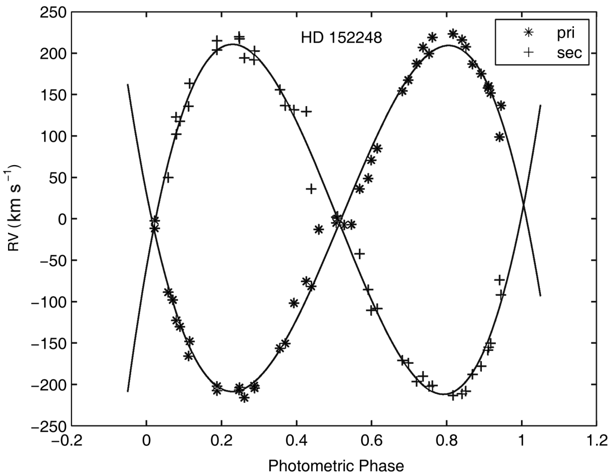

Fig. 5 Radial velocities of the primary and secondary components of HD 152248 plotted against the photometric phase. The observational data have been measured by Sana et al. (2001).

Note that the Gaussian errors of the orbital parameters in Table 1 are produced by the same steps for generating the $V_{\rm R}$ curves, i.e. $\Delta\gamma = 1, \Delta K = 1, \Delta e = 0.001$ and $\Delta\omega = 5$. These are close to the observational errors reported in the literature. Regarding the estimated errors, following Specht (1990), the error of the decision boundaries depends on the accuracy with which the underlying Probability Density Functions (PDFs) are estimated. Parzen (1962) proved that the expected error gets smaller as the estimate is calculated from a progressively larger data set. This definition of consistency is particularly important since it means that the true distribution will be approached in a smooth manner. Specht (1990) showed that a very large value of the smoothing parameter would cause the estimated errors to be Gaussian regardless of the true underlying distribution and that the

Table 2 Combined Spectroscopic Elements of HD 89959, HD 143705, HD 146361, HD 165052 and HD 152248

Name	Parameter	This Paper	Other paper	Reference
HD 89959	$m_{\rm p}\sin^3 i/M_\odot$	0.3110 ± 0.0003	0.3092 ± 0.0013	
	$m_{\rm s}\sin^3 i/M_\odot$	0.3038 ± 0.0002	0.3065 ± 0.0012	
	$(m_{\rm p}+m_{\rm s})\sin^3 i/M_\odot$	0.6148 ± 0.0005	—	
	$a_{\rm p}\sin i/10^6$ km	6.0849 ± 0.1430	6.125 ± 0.010	Griffin & Filiz Ak (2010)
	$a_{\rm s}\sin i/10^6$ km	6.2298 ± 0.1429	6.179 ± 0.010	
	$(a_{\rm p}+a_{\rm s})\sin i/10^6$ km	12.3147 ± 0.2859	—	
	$m_{\rm p}/m_{\rm s}$	1.0238 ± 0.0005	1.0088 ± 0.0023	
HD 143705	$m_{\rm p}\sin^3 i/M_\odot$	0.4736 ± 0.0003	0.467 ± 0.003	
	$m_{\rm s}\sin^3 i/M_\odot$	0.4645 ± 0.0003	0.461 ± 0.003	
	$(m_{\rm p}+m_{\rm s})\sin^3 i/M_\odot$	0.9381 ± 0.0006	—	
	$a_{\rm p}\sin i/10^6$ km	5.8992 ± 0.1150	5.889 ± 0.016	Griffin & Filiz Ak (2010)
	$a_{\rm s}\sin i/10^6$ km	6.0149 ± 0.1149	5.963 ± 0.016	
	$(a_{\rm p}+a_{\rm s})\sin i/10^6$ km	26.8271 ± 0.2299	—	
	$m_{\rm p}/m_{\rm s}$	1.0196 ± 0.0003	1.013 ± 0.004	
HD 146361	$m_{\rm p}\sin^3 i/M_\odot$	0.1316 ± 0.0005	0.126	
	$m_{\rm s}\sin^3 i/M_\odot$	0.1276 ± 0.0005	0.122	
	$(m_{\rm p}+m_{\rm s})\sin^3 i/M_\odot$	0.2593 ± 0.0010	—	
	$a_{\rm p}\sin i/10^6$ km	1.0034 ± 0.0157	0.994	Bakos (1984)
	$a_{\rm s}\sin i/10^6$ km	1.0347 ± 0.0157	1.024	
	$(a_{\rm p}+a_{\rm s})\sin i/10^6$ km	2.0381 ± 0.0313	—	
	$m_{\rm p}/m_{\rm s}$	1.0313 ± 0.0004	—	
HD 165052	$m_{\rm p}\sin^3 i/M_\odot$	1.5387 ± 0.0008	1.5 ± 0.1	
	$m_{\rm s}\sin^3 i/M_\odot$	1.3092 ± 0.0007	1.3 ± 0.1	
	$(m_{\rm p}+m_{\rm s})\sin^3 i/M_\odot$	2.8479 ± 0.0015	—	
	$a_{\rm p}\sin i/R_\odot$	5.6424 ± 0.0577	5.6 ± 0.1	Linder et al. (2007)
	$a_{\rm s}\sin i/R_\odot$	6.6312 ± 0.0576	6.6 ± 0.1	
	$(a_{\rm p}+a_{\rm s})\sin i/R_\odot$	12.2736 ± 0.1153	—	
	$m_{\rm p}/m_{\rm s}$	1.1753 ± 0.0018	1.18 ± 0.02	
HD 152248	$m_{\rm p}\sin^3 i/M_\odot$	23.3767 ± 0.0016	23.19 ± 1.19	
	$m_{\rm s}\sin^3 i/M_\odot$	23.7044 ± 0.0016	23.44 ± 0.73	
	$(m_{\rm p}+m_{\rm s})\sin^3 i/M_\odot$	47.0810 ± 0.0032	—	
	$a_{\rm p}\sin i/R_\odot$	24.7226 ± 0.1107	24.59 ± 0.17	Sana et al. (2001)
	$a_{\rm s}\sin i/R_\odot$	24.3808 ± 0.1108	24.35 ± 0.62	
	$(a_{\rm p}+a_{\rm s})\sin i/R_\odot$	49.1035 ± 0.2215	—	
	$m_{\rm p}/m_{\rm s}$	0.9862 ± 0.0001	0.990 ± 0.023	

misclassification rate is stable and does not change dramatically with small changes in the smoothing parameter.

The combined spectroscopic elements including $m_{\rm p}\sin^3 i$, $m_{\rm s}\sin^3 i$, $(m_{\rm p}+m_{\rm s})\sin^3 i$, $(a_{\rm p}+a_{\rm s})\sin i$ and $m_{\rm s}/m_{\rm p}$ are calculated by substituting the estimated parameters K, e and ω into equations (3), (15) and (16) in Karami & Teimoorinia (2007), where p is for the primary star and s is for the secondary star in the binary system. The results obtained for the five systems are tabulated in Table 2, and they show that our results are in good agreement with those obtained by Griffin & Filiz Ak (2010) for HD 89959 and HD 143705, Bakos (1984) for HD 146361, Linder et al. (2007) for HD 165052 and Sana et al. (2001) for HD 152248. Here the errors of the combined spectroscopic elements in Table 2 are obtained by the help of errors in the orbital parameters, such as equations (3), (15) and (16) in Karami & Teimoorinia (2007).

4 CONCLUSIONS

A PNN used to derive the orbital elements of spectroscopic binary stars was applied. PNNs are used in both regression (including parameter estimation) and classification problems. However, one can discretize a continuous regression problem to such a degree that it can be represented as a classification problem (Specht 1988, 1990), as we did in this work.

Using the measured $V_{\rm R}$ data of HD 89959, HD 143705, HD 146361, HD 165052 and HD 152248 obtained by Griffin & Filiz Ak (2010), Bakos (1984), Linder et al. (2007), and Sana et al. (2001), respectively, we find the orbital elements of these systems with the PNN. Our numerical results show that the results obtained for the orbital and spectroscopic parameters are in good agreement with those obtained by others using more traditional methods.

This method is applicable to orbits of all eccentricities and inclination angles. In this method the time taken is considerably less than the method of Lehmann-Filhés. It is also more accurate as the orbital elements are deduced from all points of the velocity curve instead of only four in the method of Lehmann-Filhés. The present method enables one to vary all of the unknown parameters γ, K, e and ω simultaneously instead of one or two of them at a time. It is possible to make adjustments in the elements before the final result is obtained. There are some cases, for which the geometrical methods are inapplicable, and in these cases the present one may be found useful. One such case would occur when observations are incomplete because certain phases could not have been observed. Another case where this method is useful is that of a star attended by two dark companions with commensurable periods. In this case, the resultant velocity curve may have several unequal maxima and the geometrical methods fail altogether.

References

Bakos, G. A. 1984, AJ, 89, 1740
Bazarghan, M., Safari, H., Innes, D. E., Karami, E., & Solanki, S. K. 2008, A&A, 492, L13
Griffin, R. F., & Filiz Ak, N. 2010, Ap&SS, 330, 47
Karami, K., & Mohebi, R. 2007a, ChJAA (Chin. J. Astron. Astrophys.), 7, 558
Karami, K., & Mohebi, R. 2007b, Journal of Astrophysics and Astronomy, 28, 217
Karami, K., & Mohebi, R. 2009, Journal of Astrophysics and Astronomy, 30, 153
Karami, K., Mohebi, R., & Soltanzadeh, M. M. 2008, Ap&SS, 318, 69
Karami, K., & Teimoorinia, H. 2007, Ap&SS, 311, 435
Lehmann-Filhés, R. 1894, Astronomische Nachrichten, 136, 17
Linder, N., Rauw, G., Sana, H., De Becker, M., & Gosset, E. 2007, A&A, 474, 193
Parzen, E. 1962, Annals of Mathematical Statistics, 33, 1065
Petrie, R. M. 1962, Astronomical Techniques, ed. W. A. Hiltner (Chicago: Univ. of Chicago Press)
Sana, H., Rauw, G., & Gosset, E. 2001, A&A, 370, 121
Smart, W. M. 1990, Textbook on Spherical Astronomy, ed. R. M. Green (Cambridge Univ. Press), 360
Specht, D. F. 1988, in Proceedings of the IEEE International Conference on Neural Networks (San Diego), 2427 July, 525
Specht, D. F. 1990, Neural Networks, 3, 109
Sterne, T. E. 1941, Proceedings of the National Academy of Science, 27, 175